

RESEARCH

Open Access



Doxycycline-integrated silk fibroin hydrogel: preparation, characterizations, and antimicrobial assessment for biomedical applications

Kranti Kiran Reddy Ealla^{1,2*}, Chandra Sri Durga³, Vikas Sahu², Neema Kumari⁴, Jayachandran Venkatesan⁵, Vishnu Priya Veerarahavan⁶, Pratibha Ramani⁷, Kiran Kumar Bokara^{8*} and Karthikeyan Ramalingam²

Abstract

Background Tooth extraction, a common dental procedure, is often accompanied by pain, trismus, and swelling due to alveolitis caused by oral bacteria. Doxycycline is prescribed to alleviate infection and improve socket healing, but its immediate absorption in the bloodstream makes the treatment less effective at oral sites. This emphasizes the importance of a drug delivery system to gradually slow its release at the oral wound site and increase its bioavailability to make the treatment effective over time.

Methods Silk fibroin (SF) - doxycycline hyclate (DH) hydrogel was developed and subsequently characterized for gelation kinetics, swelling, stress-strain analysis, morphology using scanning electron microscopy, interaction between SF and DH using Fourier transform infrared (FT-IR) spectroscopy, drug release profile, antibacterial efficacy, and biocompatibility studies.

Results The results indicated that the SF-DH hydrogel maintained its structural integrity, tolerated stress and strain, and featured interconnected pores, confirming DH integration within the SF matrix. The SF-DH hydrogel formed within 8 h with the pore size range of 20–150 μm and 90.72 kPa Young's modulus. The drug release profile showed the increased release of DH up to 2 h, followed by sustained release till 8 h. The zone of inhibition was smaller with SF-DH hydrogels compared with DH for both *Staphylococcus aureus* and *Streptococcus mutans*. Furthermore, MC3T3-E1 cells showed 90% viability with SF-DH hydrogel.

Conclusions The findings suggest that SF-DH hydrogel showed sufficient mechanical strength, pore size, antimicrobial activity, and biocompatibility. Further in vivo and clinical tests are required to prove its efficacy in effective socket healing.

Keywords Antimicrobials, Biocompatible, Controlled drug delivery, Doxycycline, Hydrogel, Silk fibroin

*Correspondence:

Kranti Kiran Reddy Ealla
drekk@yahoo.co.in
Kiran Kumar Bokara
bokarakiran@ccmb.res.in

Full list of author information is available at the end of the article



© The Author(s) 2025. **Open Access** This article is licensed under a Creative Commons Attribution-NonCommercial-NoDerivatives 4.0 International License, which permits any non-commercial use, sharing, distribution and reproduction in any medium or format, as long as you give appropriate credit to the original author(s) and the source, provide a link to the Creative Commons licence, and indicate if you modified the licensed material. You do not have permission under this licence to share adapted material derived from this article or parts of it. The images or other third party material in this article are included in the article's Creative Commons licence, unless indicated otherwise in a credit line to the material. If material is not included in the article's Creative Commons licence and your intended use is not permitted by statutory regulation or exceeds the permitted use, you will need to obtain permission directly from the copyright holder. To view a copy of this licence, visit <http://creativecommons.org/licenses/by-nc-nd/4.0/>.

Introduction

Tooth extraction is one of the most common dental procedures and frequently leaves a wound in the tooth socket to heal. The alveolar bone and surrounding soft tissues undergo sequential changes to heal the socket wound [1]. This condition is often associated with pain, trismus, and swelling, which are aggravated by alveolitis (dry socket) [1–3]. Alveolitis is an inflammatory reaction caused by specific microbes in the extraction sockets. Therefore, antibiotics, such as doxycycline hyclate (DH), are prescribed to inhibit oral bacteria and enhance socket healing [3].

DH is a broad-spectrum antibiotic [4–6] belonging to the tetracycline class of drugs [6, 7] and it is largely used in dentistry [8–10]. Despite its beneficial properties, DH is completely absorbed in the bloodstream after oral intake with a bioavailability range of 73–100% [11–13] thus making treatment ineffective in healing oral wounds. Therefore, it is necessary to slow its release at the oral wound site to make healing effective gradually over time. Controlled and sustained release of a drug over an extended period requires a drug delivery system that helps sustain a constant plasma concentration at the therapeutic site [14] and prevent frequent clinical visits.

Localized drug delivery has advantages in promoting vascularization and improving cellular activity. Sustainable and controlled drug delivery has the benefit of minimizing drug usage. The additional benefits of providing the drug in the targeted area are improving its efficacy, protecting against drug degradation, and reducing side effects. Localized and targeted delivery can be achieved through various formulations, including hydrogels, nanoparticles, nanofibers, micelles, microneedles, and liposomes [15]. Of the several drug delivery systems available, silk-based drug delivery systems are the most promising owing to their unique properties, such as high environmental stability, biocompatibility, non-toxicity, and good mechanical properties [16–19]. Silk (especially silk fibroin (SF)) has been investigated as a drug delivery system for several agents, such as small molecules, proteins, and anticancer drugs [20–23]. Several drugs have been studied for controlled delivery using silk carriers, such as paclitaxel [24, 25], doxorubicin [26], and curcumin [27]. DH has been incorporated into various matrixes, including nanoparticles, nanofibrous membranes, hydrogel membranes, gelling powder, microspheres, and films. These matrixes comprise polymeric substances, including chitosan [28], hyaluronic acid [29], polycaprolactone/polyvinyl alcohol/chitosan [30], collagen [31], and gelatin [32, 33]. SF has advantages over other polymeric systems due to its greater cell adhesion capacity, biocompatibility, biodegradability, and inexpensive material [34].

SF combined with antibiotics is one of the best approaches to delivering drugs to the desired location. The advantages of adding antibiotic drugs to SF include reducing side effects and sustainably releasing drugs. Tunable delivery is an advantage of SF because it minimizes drug usage and the toxic nature of the drugs. SF combined with other materials incorporated with several antibiotics, including amoxicillin trihydrate, ciprofloxacin hydrochloride, colistin, gentamicin, levofloxacin, tetracycline hydrochloride, and vancomycin hydrochloride, is used for wound dressing, drug delivery, and orthopedic applications [35]. Drug release varies depending on the nature of the disease or its conditions. Antibiotics released from SF vary from a few hours to days, depending on the materials used along with SF.

In the current study, SF-DH hydrogel was developed, characterized, and evaluated for its antimicrobial efficacy. The SF-DH hydrogel was physiochemically characterized by gelation kinetics, swelling, stress-strain analysis, morphology, FT-IR, drug release profile, antibacterial efficacy, and biocompatibility studies to ensure its suitability as a controlled-DH delivery system.

Materials & methods

SF extraction

Bombyx mori silk cocoon shells (2 g), obtained from the Government Cocoon Market Hyderabad (Central Silk Board, India), were cut into small pieces and boiled to degum at 90 °C in 0.02 M sodium carbonate (Na_2CO_3) (Sigma Aldrich, Catalog#S77795) for 15 min with continuous stirring. Shells were squeezed adequately to remove the solution and boiled again in 0.02 M Na_2CO_3 as mentioned previously.

After degumming, the silk fibres were rinsed three times with distilled water to remove traces of Na_2CO_3 . The excess water was then squeezed out, and the SF was dried overnight at 60 °C in a hot-air oven. Next, 1 g of the dried fibres were dissolved in freshly prepared 9.3 M lithium bromide (LiBr) (Sigma Aldrich, Catalog#746479) solution at 60 °C for 4 h. To remove LiBr, the SF was dialysed in a dialysis bag (Himedia, Catalog#LA401) with ultrapure water for 72 h. The water in the dialysis bag was changed every 1, 2, 4, 8, 12, 24, 36, 48, and 60 h. After dialysis, the SF was centrifuged at 9000 rpm for 20 min at 4 °C. The supernatant containing purified SF was collected. SF concentration was calculated using weight/volume (w/v) measurements.

Gelation kinetics

The gelation kinetics were determined by optical density (OD) changes in the SF-DH mixture. SF (125 μL , (5% w/v)) was added to the wells of a 96-well plate with different amounts of DH (Sigma Aldrich, Catalog#D9891) (1, 2, 3, 4, and 5 mg) using 100 $\mu\text{g}/\mu\text{L}$ stock solution. SF-DH

mixture was thoroughly mixed in each well. The plate was then incubated at 37 °C. OD readings were taken at 550 nm using a multi-plate reader (Tecan – Infinite M-200Pro) every 60 min for 20 h.

SF-DH hydrogel preparation

The SF-DH hydrogel was prepared by mixing 125 µL SF solution and 20 µL DH (100 µg/µL stock solution). The hydrogel formed instantaneously upon mixing and was left at room temperature for 8 h for stabilisation. Subsequently, the hydrogel was shifted to 4 °C for 3 days for further stabilisation. Thereafter, it was placed at -80 °C overnight. The frozen hydrogel was lyophilized to remove excess water, thus generating a dry hydrogel for subsequent experiments.

Swelling study

The dry lyophilized SF-DH hydrogels ($n=3$) were weighed and then immersed in distilled water at 37 °C. Weight and diameters of wet hydrogels were measured, after removing excess water with blotting paper, at different time points for up to 12 h. After measurement at each time point, hydrogels were placed back in the water each time. The swelling % by mass and diameter were calculated using Eq. 1 and Eq. 2, respectively [36].

Equation 1. Swelling % by mass

$$S (\%) = \frac{M_t - M_0}{M_0} \times 100$$

Where M_t is the mass of the hydrogel at time t and M_0 is the mass at time 0.

Equation 2. Swelling % (SR) by diameter calculation

$$S (\%) = \frac{d_t - d_0}{d_0} \times 100$$

Where d_t is the diameter of the hydrogel at time t and d_0 is the diameter at time 0.

Stress and strain study

SF-DH hydrogels were prepared in a 5 ml Eppendorf tube for the compression tests. The test was carried out to obtain stress-strain curves to determine the elastic modulus and elastic limit of SF-DH using a mechanical testing device (IMADA Model No: ZTA-500 N) at a 2 mm/min velocity [37, 38].

Scanning electron microscopy

Lyophilized samples were mounted on a sample tube and coated with gold-palladium (Au: Pd 80:20) using a sputter coater. The prepared samples were then examined using

a Scanning Electron Microscope (SEM) (S3700N, HITACHI, Japan) at an accelerating voltage of 20 kV using a secondary electron (SE) detector. Micrographs were taken at a magnification of 100 x.

Fourier transform infrared (FTIR) spectroscopy

The infrared spectra of SF, DH, and lyophilized SF-DH hydrogels were analysed using FTIR spectroscopy (FTIR-7600). Room-temperature FTIR spectra were recorded on solid samples in potassium bromide pellets with a resolution of 4 cm^{-1} . The measurements were performed in the 400–4000 cm^{-1} range with a frequency of 64 times.

Entrapment efficiency and drug release profile

SF-DH hydrogels ($n=3$) were added to an Eppendorf tube with 1 ml of 0.9% saline and placed in a shaker incubator (REMI, Catalog#RH180) at 37 °C and 50 rpm. At specific intervals, aliquots of 1 ml were taken from each tube and replaced with fresh saline. The collected samples were centrifuged at 3000 rpm for 5 min. One hundred microliters of the sample were added to High-Performance Liquid Chromatography (HPLC) vials.

Chromatographic separation: The analysis was performed using a mobile phase of 55% acetic acid (5%), 25% acetonitrile, and 20% methanol. The separation was performed on a C18 chromatographic column with dimensions of 4.6 mm internal diameter and 250 mm length, packed with 5 µm particles. The operating conditions were set at 15 °C and a 1 ml/min flow rate. A sample volume of 25 µL was injected, and the sample components were detected at a wavelength of 347 nm. The average of the samples is plotted on the graph.

The entrapment efficiency of the drug in the hydrogel was calculated using the HPLC method using the following equation [39]:

Equation 3, Encapsulation Efficiency (%)

$$\text{Entrapment Efficiency (\%)} = \frac{\text{Amount of drug in the hydrogel (mg)}}{\text{Initial amount of drug (mg)}} \times 100$$

Zone of inhibition

Staphylococcus aureus and *Streptococcus mutans* were cultured in nutrient broth (Himedia, Catalog#MM244) at 37 °C and 200 rpm overnight. *S. aureus* culture was spread on nutrient agar (Himedia, Catalog#MM012), and *S. mutans* culture was spread on Mutans Sanguis Agar (Himedia, Catalog#M977). A puncture was made using a gel borer at the centre of the agar plates. SF (125 µL), DH (20 µL of 100 µg/µL stock solution), and SF-DH hydrogels were placed in the punctures of their respective plates. The plates were then incubated at 37 °C for 24 h. The zone of inhibition was calculated by measuring the diameter of the zone of inhibition.

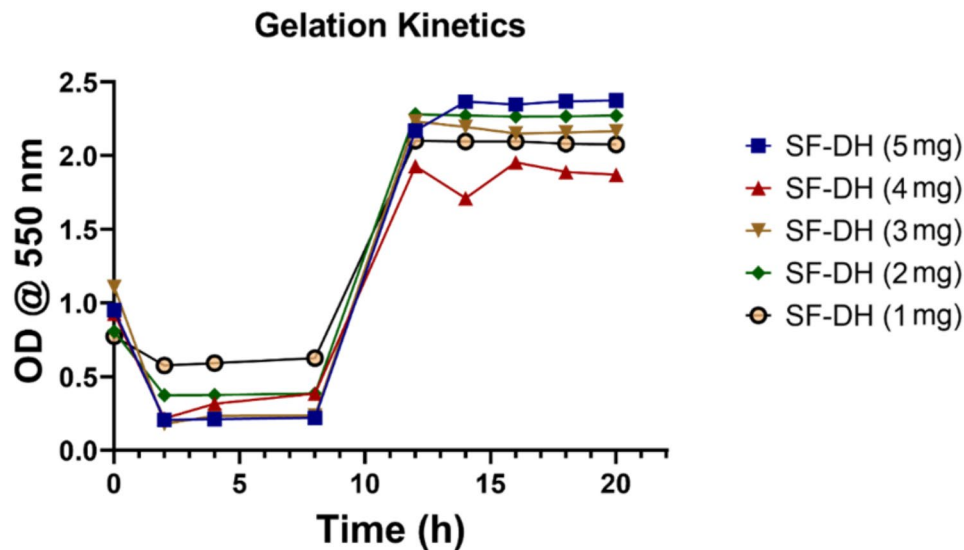


Fig. 1 SF-DH hydrogel gelation kinetics. Higher gelation kinetics were observed with 5 mg DH

Biocompatibility studies

MC3T3-E1 mouse preosteoblast was procured from the American Type Culture Collection (ATCC-CRL 2593). The obtained cells were cultured in Minimal Essential Medium-alpha (α -MEM) (Himedia- AL221A) at 37 °C in a 5% CO₂ atmosphere. The media used in this study were prepared by adding 10% (v/v) fetal bovine serum (FBS; Himedia, RM10681) and 1% penicillin/streptomycin (Himedia, A007) [40]. The cells were seeded into the 96 plates (1×10^4 cells/well) and incubated at 37 °C and 5% CO₂. After the cells were 60% confluent, SF, DH, and SF Hydrogels were added to each well. The control was the cells without sample treatment. The plates were incubated at 37 °C and 5% CO₂ for 24 h. Media was aspirated from the well, and MTT solution was added and incubated for 4 h. The MTT solution was removed, and 100 μ L of DMSO was added to each well. The absorbance of the solution was measured at 570 nm. Cell viability was calculated against control.

Statistical analysis

All experimental data were expressed as the mean \pm standard deviation (SD) of a minimum of three replicates for each hydrogel in every experiment. Origin Lab and GraphPad Prism 8.0. software used to draw the graphs and statistical analysis.

Results

Gelation profile

Gelation kinetics results (Fig. 1) showed that after 8 h, there was an increase in the absorbance of all the SF-DH hydrogels, with the highest absorbance in the SF hydrogel with 5 mg DH. Hydrogel with 1–3 mg of DH followed a similar pattern as that of 5 mg DH, with 2 mg showing

Table 1 The absorption of the water content of the dehydrated SF-DH hydrogel was maintained in deionised water at different time (h) intervals

Time	Net weight (mg)	Swelling % by mass	Diameter (mm)	Swelling % by diameter
0	8.75	0	9	0
20 s	50	471.43	9	0
1 h	52	494.28	9	0
2 h	55	528.57	9	0
3 h	55	528.57	9	0
4 h	55	528.57	9	0
6 h	50	471.43	9	0
12 h	50	471.43	9	0

relatively similar gelation kinetics though less than 5 mg DH. However, with 4 mg DH, gelation kinetics was the least.

Swelling profile

Table 1 presents the swelling profiles of SF-DH hydrogels. The initial dry gel weight was 8.75 mg. After adding water, the swelling % increased during the initial hours. After 2 h, the swelling % increased by 528.57%. Subsequently, after 4 h, the gel was saturated, and after that, weight started decreasing.

Stress and strain profile

The stress-strain curve of the SF-DH hydrogel is shown in Fig. 2. From the graph, Young's modulus for the formulated hydrogel was 90.72 kPa.

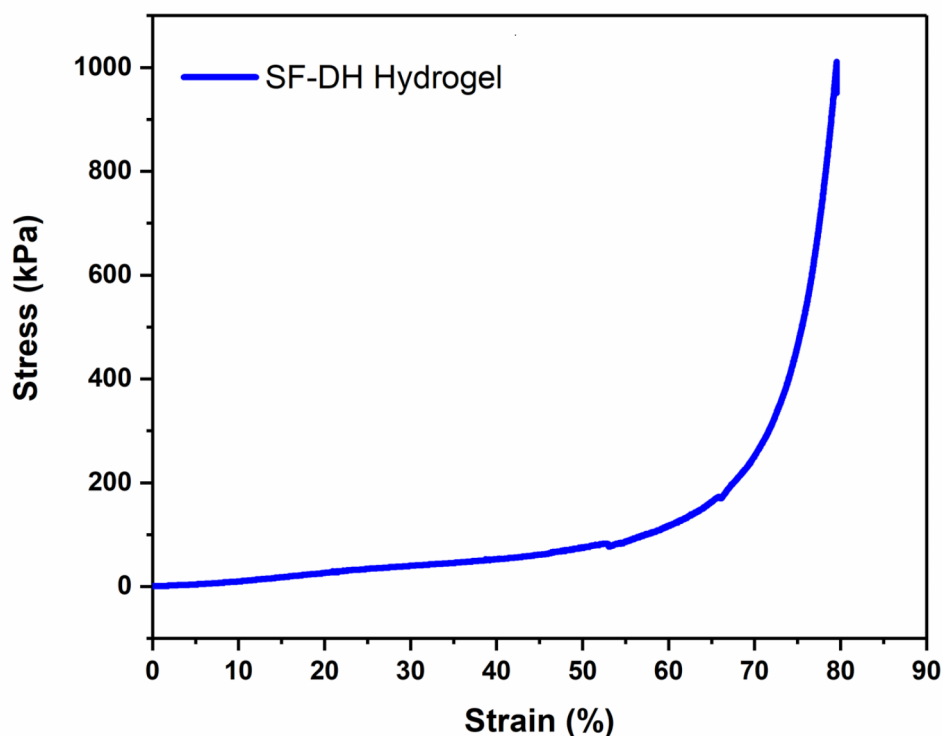


Fig. 2 The graph represents the stress-strain of the SF-DH hydrogel

Topological analysis

Morphological analysis of the SF, DH, and SF-DH hydrogels was performed using SEM. Figure 3 shows SEM images, revealing the distinct characteristics of each. Figure 3 A shows randomly entangled SF threads, while Fig. 3B shows DH's irregular cylindrical and cubical crystalline morphologies. In contrast, SF-DH hydrogel showed multiple interconnected pores of varying sizes (20 μm to 150 μm) (Fig. 3C).

FTIR profile

The SF-DH hydrogel exhibited peaks (Fig. 4) similar to those of the control SF protein and DH. FT-IR spectra of SF-DH hydrogel showed the characteristic vibration bands around 3279 cm^{-1} having N-H and O-H stretching, 1626 cm^{-1} was assigned to the absorption peak of the peptide backbone of amide I (C=O stretching), bands around 1521 cm^{-1} to amide II (N-H bending), the bands around 1235 cm^{-1} to amide III (C-N stretching).

In addition, the addition of DH in SF shifts the bond peak from 1620 cm^{-1} to 1626 cm^{-1} . DH peaks are not visible in the SF hydrogel due to the addition of a trace level of the drug in the protein structure.

Entrapment efficiency and drug release profile

The release profile revealed that DH release increased gradually, and the complete drug was released by 8 h (Fig. 5). The drug-entrapment efficiency of the prepared

SF-DH hydrogel was 99.9%. SF hydrogels can load all added drugs into their matrix [15].

Zone of inhibition with SF-DH hydrogel

A clear zone of inhibition was observed (Fig. 6) for both *S. aureus* and *S. mutans* with the SF-DH hydrogel and DH alone. SF-DH hydrogel had a smaller zone of inhibition (13 mm) against *S. aureus* as compared to DH alone, which was 17 mm (Fig. 6A). In contrast, in the case of the *S. mutans* bacterial strain, the antibacterial efficacy of the SF-DH hydrogel was found to be 8 mm when compared with that of DH alone, which was 11 mm (Fig. 6B). SF showed no inhibitory effect against *S. aureus* or *S. mutans*, indicating antibacterial activity solely from DH. The antimicrobial mechanism of DH is shown in the Fig. 6 (II).

Biocompatibility studies SF-DH hydrogel

MC3T3-E1 cells showed viability of 80.3% and 90.3%, with SF and SF-DH, respectively. With DH, the cell viability was 39.7%.

Discussion

In this study, SF-DH hydrogel was developed and characterized to test its efficacy in the controlled release of DH. The study showed sufficient mechanical strength and controlled drug release with suitable pore sizes, antimicrobial efficacy, and biocompatibility.

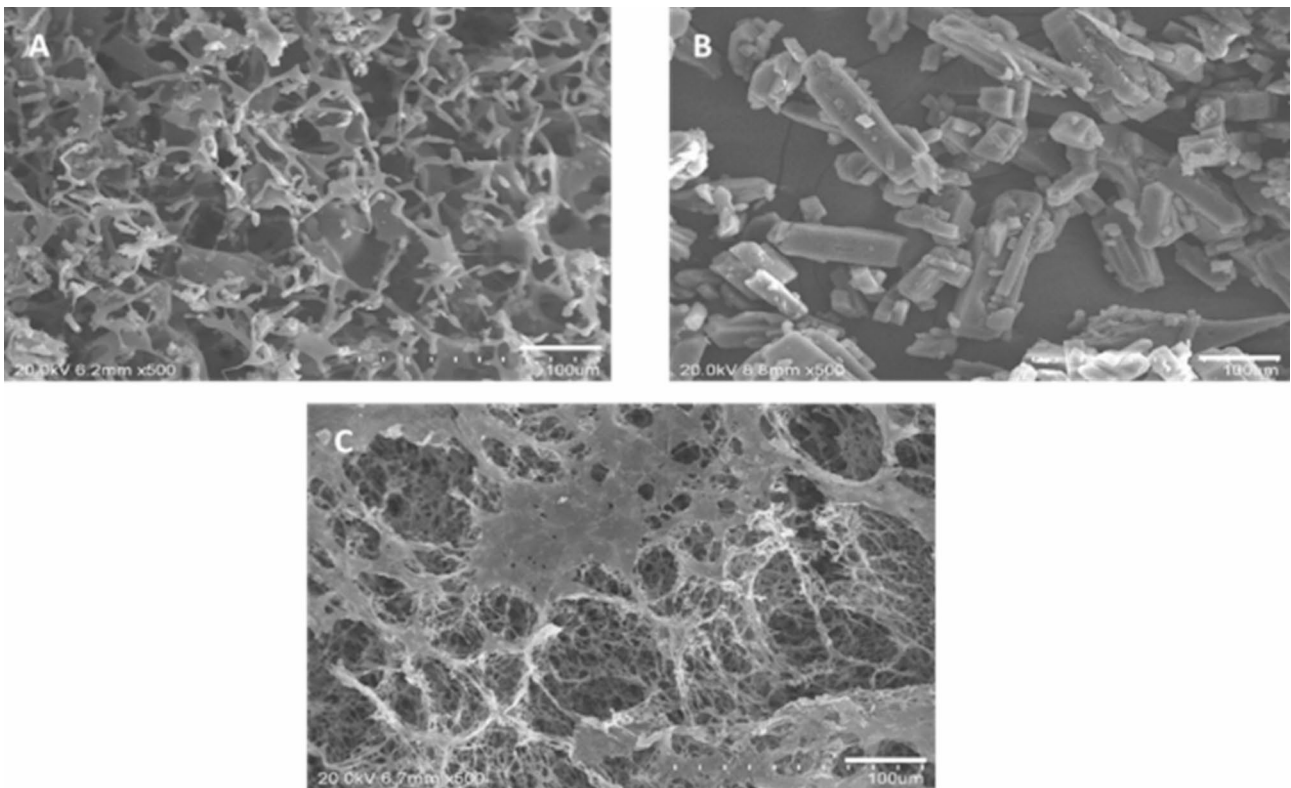


Fig. 3 Topological analysis of (A) SF, (B) DH, and (C) SF-DH hydrogel by SEM. Scale bar: 100 μm

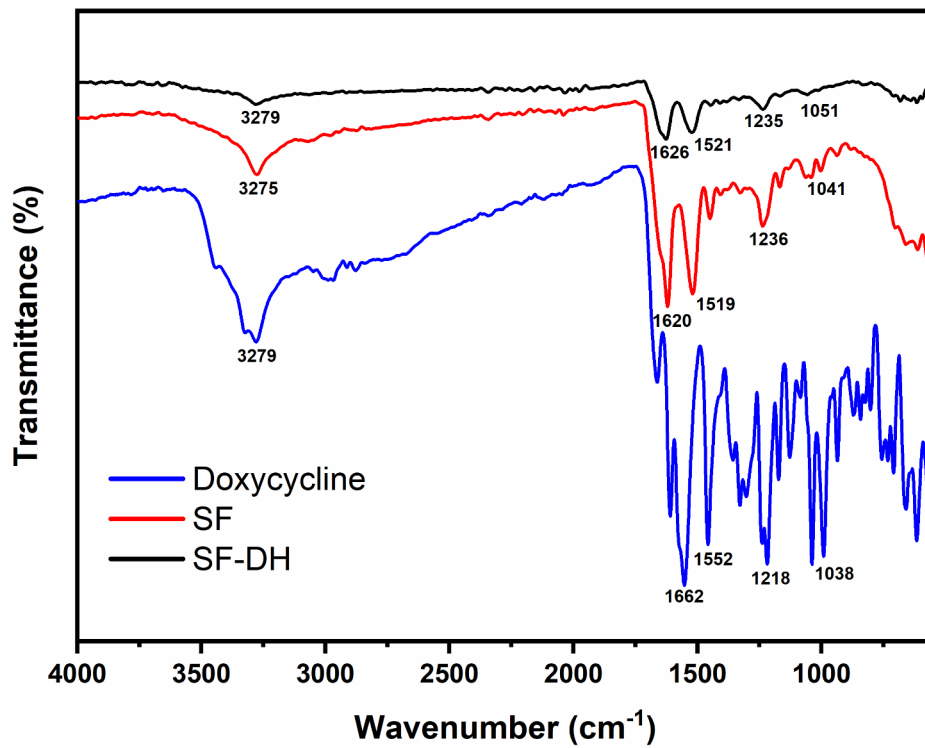


Fig. 4 FTIR spectra of SF protein, DH, and SF-DH hydrogel

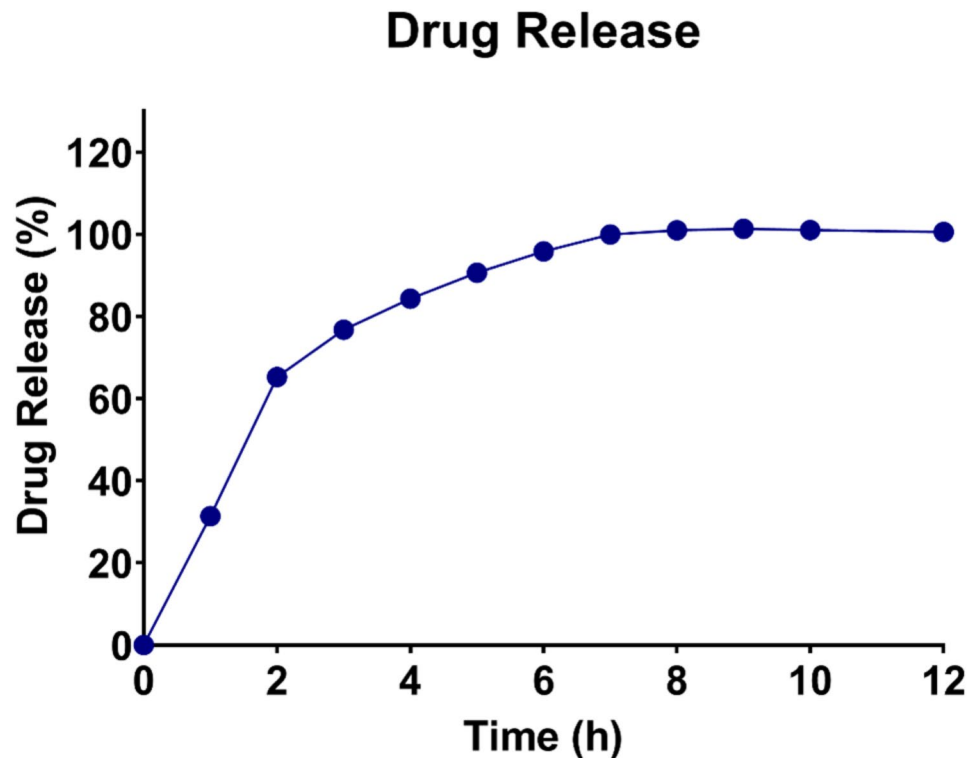


Fig. 5 Release profile of DH from DH-SF hydrogel. A gradual increase in the release of DH was observed for up to 4 h

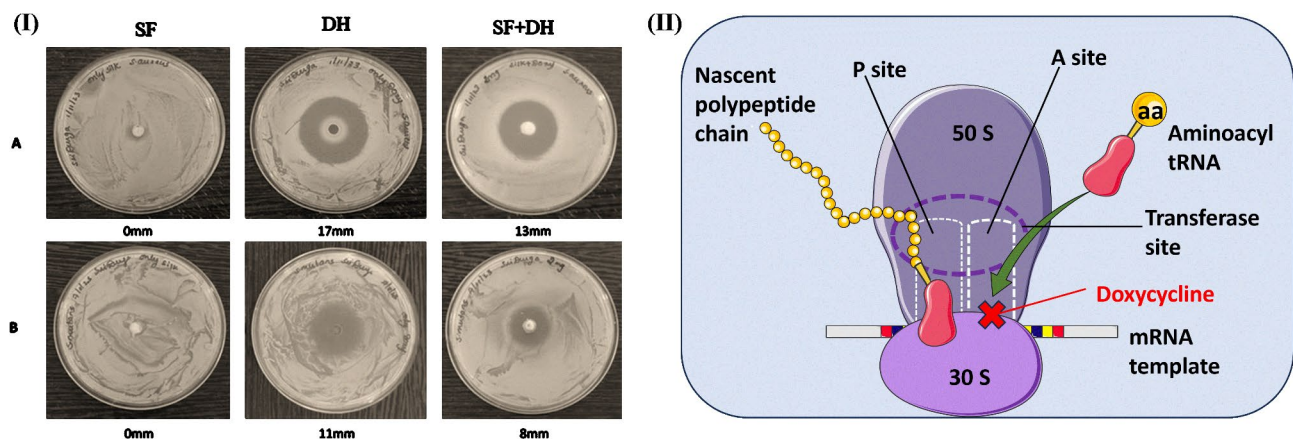


Fig. 6 (I) Zone of inhibition. With the SF-DH hydrogel, the zone of inhibition was smaller than that with DH alone in both (A) *S. aureus* and (B) *S. mutans* and (II) Antimicrobial mechanism of DH

Gelation kinetics revealed that the interaction between SF and DH resulted in the immediate formation of a hydrogel by SF, which was difficult to achieve without the addition of DH. Usually, physical or chemical cross-linkers are used to prepare SF hydrogels, following which drugs are loaded into the hydrogel. However, our study showed that SF hydrogel was formed immediately upon adding DH, thus skipping the need for a cross-linker. The hydrogel-forming ability of DH may be due to the interaction between amine and carboxylic acid groups of SF and the other hydrophilic substances of DH.

The swelling behavior is an important parameter to consider in soft tissue engineering applications. The swelling behavior of hydrogels helps improve nutrient supplementation to the cells, and cells can proliferate through the pores, which can help regenerate the tissue. Hydrogels can be categorized as high-swelling hydrogel, non-swelling hydrogel, and shrinkable hydrogel. The non-swelling hydrogel has pore size, interconnected porosity, and volume of the scaffolding system [36]. In this study, the initial absorption of water and its gradual loss with a 0% swelling ratio of hydrogel indicated the hydrogel's

ability to retain its structural integrity over time. Water uptake and water retention with swelling ratio play an important role in developing socket preservation materials. The net weight starts to decrease after 4 h, and it may be due to the release of drugs and the disruption of the hydrogel system.

A study evaluating the application of hydroxyapatite-SF-alginate hydrogel as a dental scaffolding material found Young's modulus of the hydrogel ranging from 40 ± 20 kPa to 100 ± 20 kPa [41]. The Young's modulus of the SF-DH hydrogel in this study falls within this range, which is 90.72 kPa, indicating its suitability in oral applications.

Topological analysis revealed multiple interconnected pores of variable sizes, which are necessary to improve drug release [42]. This interconnected porosity is also useful for tissue regeneration and nutrient supplements. The varying pore sizes of the hydrogel in the study could be attributed to the freeze-dried technique which generates scaffolds that are highly porous and interconnected with high surface area, and they preserve the native structure of SF from decomposition. The pore size of 100 μm to 500 μm is suitable for soft and hard tissue regeneration [43]. In this study, the pore size of the hydrogel ranged from 20 to 150 μm indicating its suitability for nutrient supply, bone regeneration, extracellular matrix formation, tissue growth, and removal of waste [43].

Fourier transform infrared spectroscopy results suggest that the characteristic bonds for amide I, amide II, and amide III are 1620 cm^{-1} , 1519 cm^{-1} , and 1236 cm^{-1} , respectively. Small shifting was observed in the amide I and amide II; the amide I peak shifted from 1260 cm^{-1} to 1266 , whereas amide II peaks shifted from 1519 cm^{-1} to 1521 cm^{-1} , confirming the presence of interaction between SF and DH hydrogel [44, 45]. The interaction may be the presence of the carboxyl and amine groups from the SF and hydrophilic groups of DH. DH peaks were not visible in the SF hydrogel because of the trace level addition in the protein structure.

Purification steps after loading drugs in SF hydrogel often lead to the loss of drugs from the hydrogel, and the entrapment efficiency is found to be around 60% [46]. However, in this study, lyophilization directly after hydrogel formation with DH led to 99.9% entrapment efficiency. This direct lyophilization step can prevent drug loss during drug delivery system preparation. Furthermore, the release of DH for up to 8 h suggests a controlled and efficient release mechanism. For example, in a study by Giovagnoli et al., DH release from alginate hydrogel microspheres was around 80–90% within 3.5 h to 4 h [13].

The antibacterial efficacy of the SF-DH hydrogel against *S. aureus* and *S. mutans* exhibited a clear zone of inhibition with a smaller zone of inhibition compared

to the zone of inhibition by DH only because the hydrogel matrix formed by SF facilitated a sustained and controlled release of DH, thereby exerting an antibacterial effect with a zone of inhibition less than the zone of inhibition with DH alone. The sustained-release mechanism appears to contribute to a more effective inhibition of bacterial growth over time. Mesoporous nanosilica-loaded DH shows better antimicrobial activity against *S. mutans*. The electrospun fibre membrane of polycaprolactone/polyvinyl alcohol/chitosan combined with DH shows sustainable drug release. It also significantly inhibits microbes such as *A. actinomycetemcomitans*, *A. viscosus*, *P. intermedia*, and *P. gingivalis*. The inhibition zone in SF-DH was lower than the DH for *S. aureus* and *S. mutans*, which might be attributed to the surface protein's limited release of the drugs, which restricts their diffusion. The inhibition of DH is higher and shows more anti-microbial activity, likely due to its hydrophilicity and ease of diffusing in the agar media. SF's absence of an inhibition zone could be due to its lack of antimicrobial activity. The drug release study and the antimicrobial assay support the antimicrobial results.

The antibacterial mechanism of DH includes inhibiting bacterial protein synthesis by allosteric binding to the 30 S prokaryotic ribosomal unit. This binding ultimately impedes the elongation phase of protein synthesis by preventing the binding of aminoacyl tRNA to mRNA, thus halting the production of essential proteins for bacterial survival and functioning [4–6]. Additionally, DH also possesses anti-inflammatory properties [4, 6, 47, 48] and mediates anti-inflammatory actions by reducing Protease-Activated Receptor 2 and matrix metalloproteinases, downregulating the nuclear factor- κB (NF- κB) pathway, and preventing calcium-dependent assembly and lymphocytic proliferation [4, 6]. It also inhibits nitric oxide synthase, an inflammatory signaling molecule [4, 6].

Furthermore, the biocompatibility of the developed SF-DH hydrogel with pre-osteoblast MC3T3-E1 cells indicates its safety for users. This study aligns with a previous study where SF showed biocompatibility with stem cells. Additionally, it also promoted the differentiation of stem cells into osteogenic lineages, providing a platform for cell growth [18].

The findings of this study are limited by the lack of a proper physiological environment and testing of an actual extraction socket to demonstrate the efficacy of DH released in a controlled and sustained manner to heal the socket over time. Therefore, cellular experiments such as polymerase chain reaction, western blotting, flow cytometry analysis, in vivo, and clinical studies are required to validate the potential of the SF-DH hydrogel for healing extraction sockets while alleviating infection. A comprehensive study of these materials' mechanical properties, long-term stability, and use of cross-linkers to

prolong drug release will also increase our understanding of their suitability for practical biomedical applications.

Conclusion

High entrapment efficiency, sufficient mechanical strength, slowed DH release, and antimicrobial and non-cytotoxicity characteristics of SF-DH hydrogel indicate its potential use in tooth extraction socket healing. Further studies are required on in vivo and clinical studies to confirm its applicability and safety in dental patients. Controlled DH release from the SF-DH hydrogel with antibacterial properties promises efficacy for socket healing after tooth extraction. By utilizing SF's biocompatibility and drug-delivery potential of SF, a foundation has been established for further research on DH to improve dental-care outcomes.

Abbreviations

α-MEM	Minimal Essential Medium-alpha
ATCC	American Type Culture Collection
DH	Doxycycline Hyclate
FBS	Fetal Bovine Serum
FT-IR	Fourier Transform Infrared (FT-IR) Spectroscopy
HPLC	High-Performance Liquid Chromatography
LiBr	Lithium Bromide
Na ₂ CO ₃	Sodium carbonate
NF-κB	Nuclear Factor-κB
OD	Optical Density
SEM	Scanning Electron Microscope
SF-DH	Silk Fibroin-Doxycycline Hyclate
SF	Silk Fibroin

Acknowledgements

The authors would like to thank Manish Kumar Tripathi, a PhD scholar at the Biomedical Engineering department of the Indian Institute of Technology Hyderabad, India, for helping in the Stress and strain study.

Author contributions

Kranti Kiran Reddy Ealla: Conceptualisation, Formal analysis, Funding acquisition, Methodology, Project administration, Resources, Supervision. Chandra Sri Durga: Data curation, Investigation. Vikas Sahu: Conceptualisation, Formal analysis, Funding acquisition, Methodology, Project administration, Resources, Supervision. Jayachandran Venkatesan: Writing—original draft, Writing - review & editing. Vishnu Priya Veeraraghavan: Formal analysis, Supervision. Karthikeyan Ramalingam: Formal analysis, Supervision; Pratibha Ramani: Formal analysis, Supervision. Kiran Kumar Bokara: Conceptualisation, Formal analysis, Methodology, Project administration, Resources, Supervision. All authors reviewed the manuscript.

Funding

This work was supported by Aasya Healthcare [AASYAHEALTH/PROJECT/2022–2023/001].

Data availability

The datasets analyzed during the current study are available from the corresponding author upon reasonable request.

Declarations

Ethical approval and consent to participate

Not applicable.

Consent for publication

Not applicable.

Competing interests

The authors declare no competing interests.

Author details

- ¹Department of Oral and Maxillofacial Pathology, Saveetha Institute of Medical and Technical Sciences, Saveetha University, Chennai 600077, India
- ²Department of Oral and Maxillofacial Pathology, Malla Reddy Institute of Dental Sciences, Malla Reddy Vishwavidyapeeth, Hyderabad 500055, India
- ³Atal Incubation Centre, Centre for Cellular and Molecular Biology, Aasya Health Care Pvt. Ltd, Hyderabad 500039, India
- ⁴Department of Microbiology, Malla Reddy Institute of Medical Sciences, Hyderabad 500055, India
- ⁵School of Dental Sciences and Technology, Department of Biomaterials and Transplant Sciences, Malla Reddy Vishwavidyapeeth, Hyderabad 500055, Telangana, India
- ⁶Centre for Molecular Medicine and Diagnostics (CoMManD), Saveetha Institute of Medical and Technical Sciences, Saveetha University, Chennai 600077, India
- ⁷Department of Oral and Maxillofacial Pathology, Saveetha Dental College & Hospitals, Saveetha University, Chennai 600077, India
- ⁸CSIR-Center for Cellular and Molecular Biology, Annexe-II, Medical Biotechnology Complex, Uppal Road, Hyderabad, Telangana 500007, India

Received: 10 December 2024 / Accepted: 29 January 2025

Published online: 01 February 2025

References

- Udeabor SE, Heseli A, Al-Maawi S, Alqahtani AF, Sader R, Ghanaati S. Current knowledge on the healing of the extraction socket: a narrative review. *Bioengineering*. 2023;10(10):1145.
- Bystedt H, Nord CE, Nordenram A. Effect of azidocillin, erythromycin, clindamycin and doxycycline on postoperative complications after surgical removal of impacted mandibular third molars. *Int J Oral Surg*. 1980;9(3):157–65.
- Rosa A, Pujia AM, Arcuri C. Investigation of alveolar osteitis and the effectiveness of laser treatment: a unified meta-analysis and review of the literature. *BMC Oral Health*. 2024;24(1):700.
- Henehan M, Montuno M, De Benedetto A. Doxycycline as an anti-inflammatory agent: updates in dermatology. *J Eur Acad Dermatol Venereol*. 2017;31(11):1800–8.
- Ranch KM, Maulvi FA, Koli AR, Desai DT, Parikh RK, Shah DO. Tailored doxycycline hyclate loaded in situ gel for the treatment of periodontitis: optimization, in vitro characterization, and antimicrobial studies. *AAPS PharmSciTech*. 2021;22(3):77. <https://doi.org/10.1208/s12249-021-01950-x>. PMID: 33595740.
- Khaing EM, Lertsuphotvanit N, Thammasut W, Rojviriyi C, Chansatidkosol S, Phattarateera S, et al. Cellulose acetate butyrate-based in situ gel comprising doxycycline hyclate and metronidazole. *Polymers (Basel)*. 2024;16(24):3477. <https://doi.org/10.3390/polym16243477>. PMID: 39771329; PMCID: PMC11728690.
- Ramachandran R, Schaefer B. Tetracycline antibiotics. *ChemTexts*. 2021;7(3):18.
- Ali M, Walboomers XF, Jansen JA, Yang F. Influence of formulation parameters on encapsulation of doxycycline in PLGA microspheres prepared by double emulsion technique for the treatment of periodontitis. *J Drug Deliv Sci Technol*. 2019;52:263–71.
- Cosgarea R, Eick S, Batori-Andronesu I, Jepsen S, Arweiler NB, Rössler R, Conrad T, Ramseier CA, Sculean A. Clinical and microbiological evaluation of local doxycycline and antimicrobial photodynamic therapy during supportive periodontal therapy: a randomized clinical trial. *Antibiotics-Basel*. 2021;10(3).
- Lertsuphotvanit N, Tuntarawongsa S, Chantadee T, Phaechamud T. Phase inversion-based doxycycline hyclate-incorporated borneol in situ gel for periodontitis treatment. *Gels*. 2023;9(7).
- de Macedo V, Meneghete BP, Koaski JC, Albuquerque AS, Fachi MM. Doxycycline for multidrug-resistant Gram-negative bacterial infection treatment: a scoping review. *J Glob Infect Dis*. 2023;15(3):95–100.
- Agwuh KN, MacGowan A. Pharmacokinetics and pharmacodynamics of the tetracyclines including glycylicyclines. *J Antimicrob Chemother*. 2006;58(2):256–65.

13. Giovagnoli S, Tsai T, DeLuca PP. Formulation and release behavior of doxycycline–alginate hydrogel microparticles embedded into pluronic F127 thermogels as a potential new vehicle for doxycycline intradermal sustained delivery. *AAPS PharmSciTech*. 2010;11(1):212–20.
14. Yucel T, Lovett ML, Kaplan DL. Silk-based biomaterials for sustained drug delivery. *J Control Release*. 2014;190:381–97.
15. Al-Musawi MH, Turki SH, Al-Naymi HAS, Al-salman SS, Boroujeni VV, Alizadeh M, Sattar M, Sharifianjazi F, Bazli L, Pajoo AMD. Localized delivery of healing stimulator medicines for enhanced wound treatment. *J Drug Deliv Sci Technol*. 2024;106212.
16. Damrongrungruang T, Siritapetawee M, Kamanarong K, Limmonthon S, Rattanathongkom A, Maensiri S, Nuchdamrong S. Fabrication of electrospun Thai silk fibroin nanofiber and its effect on human gingival fibroblast: a preliminary study. *J Oral Tissue Eng*. 2007;5(1):1–6.
17. Virlan MJR, Calenic B, Zaharia C, Greabu M. Silk fibroin and potential uses in regenerative dentistry—a systematic review. *Stoma Edu J*. 2014;1(2):108–15.
18. Melke J, Midha S, Ghosh S, Ito K, Hofmann S. Silk fibroin as biomaterial for bone tissue engineering. *Acta Biomater*. 2016;31:1–16.
19. Sun W, Gregory DA, Tomeh MA, Zhao X. Silk fibroin as a functional biomaterial for tissue engineering. *Int J Mol Sci*. 2021;22(3):1499.
20. Florczak A, Deptuch T, Lewandowska A, Penderecka K, Kramer E, Marszalek A, Mackiewicz A, Dams-Kozłowska H. Functionalized silk spheres selectively and effectively deliver a cytotoxic drug to targeted cancer cells in vivo. *J Nanobiotechnol*. 2020;18:1–18.
21. Kumari N, Pullaguri N, Sahu V, Ealla KKR. Research and therapeutic applications of silk proteins in cancer. *J Biomater Appl*. 2023;38(1):39–50.
22. Zhao Z, Li Y, Xie M-B. Silk fibroin-based nanoparticles for drug delivery. *Int J Mol Sci*. 2015;16(3):4880–903.
23. Mottaghtalab F, Kiani M, Farokhi M, Kundu SC, Reis RL, Gholami M, Bardania H, Dinarvand R, Geramifard P, Beiki D. Targeted delivery system based on gemcitabine-loaded silk fibroin nanoparticles for lung cancer therapy. *ACS Appl Mater Interfaces*. 2017;9(37):31600–11.
24. Chen M, Shao Z, Chen X. Paclitaxel-loaded silk fibroin nanospheres. *J Biomed Mater Res A*. 2012;100A(1):203–10.
25. Perteghella S, Sottani C, Coccè V, Negri S, Cavicchini L, Alessandri G, Cottica D, Torre ML, Grignani E, Pessina A. Paclitaxel-loaded silk fibroin nanoparticles: method validation by UHPLC-MS/MS to assess an exogenous approach to load cytotoxic drugs. *Pharmaceutics*. 2019;11(6):285.
26. Seib FP, Jones GT, Rnjak-Kovacina J, Lin Y, Kaplan DL. pH-dependent anticancer drug release from silk nanoparticles. *Adv Healthc Mater*. 2013;2(12):1606–11.
27. Montalbán MG, Coburn JM, Lozano-Pérez AA, Cenis JL, Villora G, Kaplan DL. Production of curcumin-loaded silk fibroin nanoparticles for cancer therapy. *Nanomaterials*. 2018;8(2):126.
28. Gjoseva S, Geskovski N, Szadzovska SD, Popeski-Dimovski R, Petruševski G, Mladenovska K, Goracinova K. Design and biological response of doxycycline loaded Chitosan microparticles for periodontal disease treatment. *Carbohydr Polym*. 2018;186:260–72.
29. Kanwal A, Iqbal A, Arshad R, Akhtar S, Razzaq S, Ahmad NM, Naz H, Shahnaz G. Formulation and evaluation of novel thiolated intra pocket periodontal composite membrane of doxycycline. *AAPS PharmSciTech*. 2019;20:1–14.
30. Mirzaeei S, Pourfarzi S, Saedi M, Taghe S, Nokhodchi A. Development of a PVA/PCL/CS-based nanofibrous membrane for guided tissue regeneration and controlled delivery of doxycycline hydrochloride in management of periodontitis: in vivo evaluation in rats. *AAPS PharmSciTech*. 2024;25(11):27.
31. Toledano-Osorio M, de Luna-Bertos E, Toledano M, Manzano-Moreno FJ, García-Recio E, Ruiz C, Osorio R, Sanz M. Doxycycline-doped collagen membranes accelerate in vitro osteoblast proliferation and differentiation. *J Periodontol Res*. 2023;58(2):296–307.
32. Stan D, Ruta LL, Bocancia-Mateescu LA, Mirica AC, Stan D, Micutz M, Brincoveanu O, Enciu AM, Codrici E, Popescu ID et al. Formulation and comprehensive evaluation of biohybrid hydrogel membranes containing doxycycline or silver nanoparticles. *Pharmaceutics*. 2023;15(12).
33. Hafiyah OA, Lastianny SP. Doxycycline incorporation into gelatin-carbonate apatite membrane as adjuvant post gingival curettage. *Malays J Med Health Sci*. 2023;19.
34. Hu J, Jiang Z, Zhang J, Yang G. Application of silk fibroin coatings for biomaterial surface modification: a silk road for biomedicine. *J Zhejiang Univ Sci B*. 2023;24(11):943–56.
35. Ghalei S, Handa H. A review on antibacterial silk fibroin-based biomaterials: current state and prospects. *Mater Today Chem*. 2022;23:100673.
36. Jahani M, Asefnejad A, Al-Musawi MH, Mohammed AA, Al-Sudani BT, Hameed Al-bahrani M, Kadhim NA, Shahriari-Khalaji M, Valizadeh H, Sharifianjazi F. Antibacterial and wound healing stimulant nanofibrous dressing consisting of soruplus and soy protein isolate loaded with mupirocin. *Sci Rep*. 2024;14(1):26397.
37. Kazemi N, Mahalati MJ, Kaviani Y, Al-Musawi MH, Varshosaz J, Bakhtiari SSE, Tavakoli M, Alizadeh M, Sharifianjazi F, Salehi S. Core-shell nanofibers containing L-arginine stimulates angiogenesis and full thickness dermal wound repair. *Int J Pharm*. 2024;653:123931.
38. Al-Sudani BT, Al-Musawi MH, Kamil MM, Turki SH, Nasiri-Harchegani S, Najafinezhad A, Noory P, Talebi S, Valizadeh H, Sharifianjazi F. Vasculo-osteogenic keratin-based nanofibers containing merwinite nanoparticles and sildenafil for skin tissue regeneration. *Int J Pharm*. 2024;667:124875.
39. Tavakoli M, Al-Musawi MH, Kalali A, Shekarchizadeh A, Kaviani Y, Mansouri A, Nasiri-Harchegani S, Kharazi AZ, Sharifianjazi F, Sattar M. Platelet rich fibrin and simvastatin-loaded pectin-based 3D printed-electrospun bilayer scaffold for skin tissue regeneration. *Int J Biol Macromol*. 2024;265:130954.
40. Chen BQ, Kankala RK, Chen AZ, Yang DZ, Cheng XX, Jiang NN, et al. Investigation of silk fibroin nanoparticle-decorated poly(L-lactic acid) composite scaffolds for osteoblast growth and differentiation. *Int J Nanomedicine*. 2017;12:1877–90. <https://doi.org/10.2147/IJN.S129526>. PMID: 28331312; PMCID: PMC5352233.
41. Chuysinuan P, Nooeaid P, Thanyacharoen T, Techasakul S, Pavasant P, Kanjanamekanant K. Injectable eggshell-derived hydroxyapatite-incorporated fibroin-alginate composite hydrogel for bone tissue engineering. *Int J Biol Macromol*. 2021;193:799–808.
42. Varghese JS, Chellappa N, Fathima NN. Gelatin–carrageenan hydrogels: role of pore size distribution on drug delivery process. *Colloids Surf B Biointerfaces*. 2014;113:346–51.
43. Jose J, Sultan S, Kalarikkal N, Thomas S, Mathew AP. Fabrication and functionalization of 3D-printed soft and hard scaffolds with growth factors for enhanced bioactivity. *RSC Adv*. 2020;10(62):37928–37.
44. Zhang Q, Zhao Y, Yan S, Yang Y, Zhao H, Li M, Lu S, Kaplan DL. Preparation of uniaxial multichannel silk fibroin scaffolds for guiding primary neurons. *Acta Biomater*. 2012;8(7):2628–38.
45. Khosravimelal S, Chizari M, Farhadhosseinabadi B, Moosazadeh Moghaddam M, Gholipourmalekabadi M. Fabrication and characterization of an antibacterial chitosan/silk fibroin electrospun nanofiber loaded with a cationic peptide for wound-dressing application. *J Mater Sci Mater Med*. 2021;32:1–11.
46. Roy TC, Ansary RH, Biswas P, Haider MA. Silk fibroin hydrogel-assisted controlled release of antifungal drug ketoconazole. *J Drug Deliv Ther*. 2023;13(3):125–30.
47. Valentín S, Morales A, Sánchez JL, Rivera A. Safety and efficacy of doxycycline in the treatment of rosacea. *Clin Cosmet Investig Dermatol*. 2009;2:129–40.
48. <http://www.antibiotics-info.org/doxycycline.html>

Publisher's note

Springer Nature remains neutral with regard to jurisdictional claims in published maps and institutional affiliations.